JOURNAL OF MATERIAL SCIENCE 29 (1994) 5859–5867

Effects of processing methods and parameters on the mechanical properties and microstructure of carbon/carbon composites

WEN-CHI CHANG[‡], CHEN-CHI M. MA*[‡§], NYAN-HWA TAI[§‡], CHUN-BIN CHEN[‡]
[‡]*Institute of Chemical Engineering, and* [§]*Materials Science Centre, National Tsing Hua University, Hsin-Chu, 30043, Taiwan*

The influence of the fabrication parameters during carbonization and densification processes on the mechanical properties and the microstructure of carbon/carbon (C/C) composites were investigated. The C/C composites were made by using phenolic resin as precursor and two-dimensional carbon fabrics as reinforcements for the first carbonization. The effects of heating rate and heat-treatment temperature during the initial carbonization process on the properties of C/C composites are presented. Further densification treatment was completed by chemical vapour infiltration (CVI) and a liquid-resin impregnation process. The CVI route was found to be more efficient than the resin-impregnation process. The interlayer spacing of C/C composites did not change after resin re-impregnation for several times. However, the interlayer spacing of the C/C composites was reduced when the processing temperature in the CVI process was increased. Higher flexural strength and flexural modulus were obtained because the densities of the composites were enhanced either by the chemical vapour infiltration process or by the resin-impregnation route. The variation in thickness of the CVI deposited carbon within the preformed composite was studied and the morphology of the fracture surface of the C/C composites was also examined.

1. Introduction

The use of composite materials for structure applications in aircraft and spacecraft industries has increased rapidly in recent years [1, 2]. Among the composites developed, C/C composites show excellent mechanical properties at extremely high temperatures that other composites cannot achieve. The applications of C/C composites are increasing, for example, as commercial brake linings in transportation vehicles as well as military aircrafts, and are adopted as leading edges of wings and nose caps in space shuttles [3, 4]. Future applications of C/C composites have been considered for supersonic aircraft of European space craft vehicles, such as *Hermes*, *Hotol*, or *Super Concorde* and for long-term application in new turbine engines [5].

The reinforcements for C/C composites are carbon or graphite fibres in the forms of unidirectional, two-directional or multi-directional [3, 4, 6]. The matrices for C/C composites are usually derived based upon two methods: chemical vapour infiltration and liquid-resin impregnation.

The fabrication of C/C composite through the deposition of PyroC via pyrolytic hydrocarbon gas within fibrous preforms at elevated temperature has been extensively studied over recent years [7–11]. The process involves the infiltration of hydrocarbon gas from the preform surface to the interior of the preform, adsorption of the gas on the fibre surface, chemical reactions and deposition of the solid product on to the fibre surface, desorption of the gas products from the fibre surface, and diffusion of the gas-phase products from the interior of the preform to the outer surface [7, 8]. The performance of C/C composites is affected by the microstructure of the deposited matrix which is significantly influenced by the processing parameters. The parameters include deposition temperature, total pressure, partial pressure of reactant, gas composition, gas flow rate, and properties of the deposition substrate [10, 11].

The liquid-impregnation method utilizes thermoset resin or thermoplastic pitch as the matrix precursor. For the C/C composites fabricated through the liquid-resin impregnation method, the combination of liquid resin and carbon fibres can serve as the starting materials for C/C composites. The process is accomplished by impregnating the liquid resin, followed by curing, carbonization and graphitization treatments of the impregnated composites. The precursor for the liquid-resin impregnation process should have a high carbon yield, which implies a low weight loss during carbonization treatment. The weight loss resulted in

* Author to whom all correspondence should be addressed.

0022–2461

TABLE I Materials used for this study

Materials	Specification	Code	Supplier
Resin	Resole-type phenolic resin, pH = 8.0–8.5, solid content 62%, viscosity at 25 °C = 100–250 cP	PF-650	Chung-Chun Plastics Co. Ltd, Taiwan
Carbon fibre	Plain weave cloth, 200 g cm^{-2}, fibre diameter 7.0 μm	TR-30 K	Mitsubishi Rayon Co. Ltd, Japan

bulk shrinkage that leads to the formation of porous voids within the composites. Densification treatment is achieved by multiple impregnation with liquid resin and subsequent recarbonization. The fabrication parameters for carbonization depend on the matrix precursor adopted. For example, coal-tar pitch causes a high carbon yield when the carbonization process is carried out in a very slow manner or under high pressure; on the other hand, thermoset resins do not require a pressure carbonization [6]. The mechanical properties of C/C composites are influenced by the matrix microstructure, fibre/matrix interface, and the post treatment between the impregnation and carbonization cycles [12, 13]. Porous C/C composites formed as a result of volatile generation and weight loss of solid materials during polymer pyrolysis. Some of the decomposed gases are trapped and generate a pressure gradient within the composites. The generation of pressure gradient with a matrix may cause cracks and voids [14].

The microstructure of the fabricated composites shows a significant influence on the properties of the composite materials [7, 8]. During the fabrication process to convert polymer composites into C/C composites, the polymer matrix is exposed to an elevated temperature environment and degradation occurs when the energy applied to the polymer network exceeds the bonding energy of the polymer network. The polymer degradation causes the generation of volatile species, weight loss, shrinkage, crack or void formation and molecular structure rearrangement. As a result, the carbonized composite becomes a porous solid material and the molecular configuration is quite different from the precursor [9, 12]. The generation of volatile species is strongly affected by carbonization processing parameters, heating rate and heat-treatment temperature, and closely related to the microstructure of carbonized composites. Several researchers show that the initial carbonization processing is one of the most important effects in the fabrication of the C/C composites [13, 14]. In order to investigate the performance of the C/C composites in detail, it is essential to understand the microstructure and mechanical property variation after first carbonization process.

The present work focused on the study of the effects of heating rate and heat-treatment temperature on the weight loss, shrinkage, density and flexural properties of C/C composites after the first carbonization. The weight gain, density and flexural properties of the C/C composites further densified through the CVI route and the liquid-resin impregnation method were also investigated.

2. Experimental procedure

2.1. Materials and sample preparation

The materials used in this study are summarized in Table I. The two-dimensional carbon fabrics were impregnated with phenolic resin using a wet winding technique and then placed in a circular air oven at 70 °C for 2 h to remove excess solvent. The impregnated fabrics were placed in a picture-frame mould and then compression moulded at 150 °C under a pressure of 135 MPa. The fabricated polymer composite plates were post-cured in a circular air oven at 150 °C for 36 h, and were cut into 50 mm × 10 mm × 1 mm test specimens using a diamond-tip saw under water cooling.

2.2. High-temperature treatment parameters

The effect of heating rate was investigated using a Linberg high-temperature tube furnace up to 1000 °C in an argon atmosphere. The heating rates were set at 30, 60, 120 and 180 °C min^{-1} and argon gas was introduced continuously into the tube furnace at a constant gas flow rate of 100 cm^3 min^{-1}.

The effect of heat-treatment temperature was investigated at 400, 600, 800, 1000 and 1200 °C in the same furnace. A heating rate of 30 °C min^{-1} was used and argon gas was also introduced continuously into the tube furnace at a constant gas flow rate of 100 cm^3 min^{-1}.

2.3. Densification by chemical vapour infiltration

The densification process of the carbonized C/C composites by isothermal chemical vapour infiltration was performed in a horizontal tube furnace. Methane was used as gas precursor of the deposited carbon, and argon was used as a carrier gas. The volume fraction of methane was 25%, and the total gas flow rate was 150 cm^3 min^{-1}. The mixture of methane gas and argon gas was channelled into the reactor after the temperature in the furnace had reached the processing temperature for 30 min.

2.4. Densification by liquid-resin impregnation

The same phenolic resin was adopted as the precursor

for C/C composites densified by liquid-resin impregnation. The viscosity of the phenolic resin was diluted to 80–100 cP by acetone. The undensified C/C composites were impregnated by the dilute resin under vacuum and then dried in a circular air oven at 70 °C for 3 h and cured in the same oven at 160 °C for 24 h. The carbonization process was performed by placing the specimens in a high-temperature tube furnace and heating them to 1000 °C under an argon atmosphere. The reimpregnation was repeated several times.

2.5. Density measurement

Composite density was measured on a Precica 180A microbalance using the water immersion method.

2.6. Weight-gain measurement

Weight gain of the composites was determined from the difference in weight between densified and undensified C/C composites. The weight of composites was measured to 0.0001 g using a Precia 180A microbalance.

2.7. Flexural properties

Flexural properties were measured using a three-point bending method with a span to depth ratio of 20 to 1 and a test speed of 1.3 mm min^{-1}. All tests were performed on an Instron testing machine model 4201. The procedures for all tests followed the ASTM D-790 method.

2.8. Microstructure evaluation

The microstructure of the carbonized composites was analysed by scanning electron microscopy (SEM). The fracture surfaces of flexural test samples were gold sputtered and examined by SEM. X-ray diffraction (XRD) was utilized to measure the d_{002} basal plane interlayer spacing. The calculation was based upon Bragg's law

$$n\lambda = 2d \sin\theta \quad (1)$$

where λ is the wavelength of the X-ray radiation, d the basal plane interlayer spacing, θ the Bragg angle, and n an integer. All specimens were analysed by copper radiation using a computer-controlled powder diffractometer at a speed of 4° min^{-1} under 40 kV and 30 mA.

3. Results and discussion

3.1. Initial carbonization process

3.1.1. Effect of heating rate

3.1.1.1. Linear Shrinkage. Fig. 1 represents the through-thickness linear shrinkage of carbonized composites fabricated at various heating rates. The shrinkages are determined from the change in dimension between uncarbonized and carbonized specimens. Results show that the dimension does not change in the fibre direction, (X-, Y-directions as illustrated in Fig. 2); however, the linear shrinkage in the Z-direction (through-thickness direction) is significantly affected by the heating rate. Because dimensions in the X-, Y-directions are controlled by the reinforced carbon fibre, the dimension of which does not change after treating at elevated temperature, no changes in the dimension of carbonized composites in the X- and Y-directions are observed in this study. On the other hand, the changes in dimension in the Z-direction of the carbonized composites are controlled by the shrinkage of the matrix; therefore, the dimension variation in the Z-direction of the composite is significantly affected by the processing parameters during carbonization.

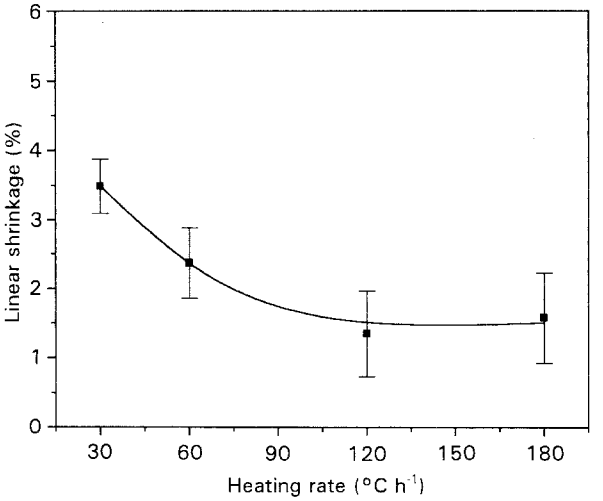

Figure 1 The through-thickness (Z-direction) linear shrinkage of first-carbonized composites with different heating rates up to a carbonization temperature of 1000 °C.

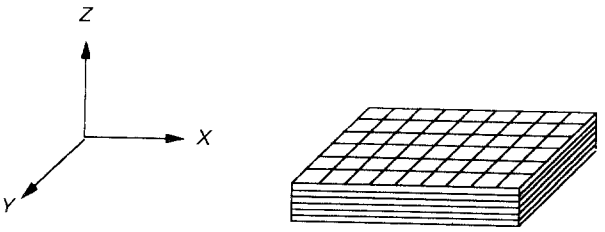

Figure 2 The coordinates of the test specimen used in this study; X-, Y-directions represent the carbon fibre direction and the Z-direction represents the through-thickness direction.

3.1.1.2. Weight loss and density change. Fig. 3 shows that the weight loss of composites is not a function of heating rate during carbonization. The dependence of the density change of the composite on the carbonization heating rate is obvious, due to the shrinkage in the Z-direction of the composite during carbonization. Fig. 4 illustrates the density change at various heating rates. The greater the shrinkage the fewer voids are formed; consequently, a denser composite material formed.

3.1.1.3. Flexural properties. The influence of heating rate on flexural strength and flexural modulus were

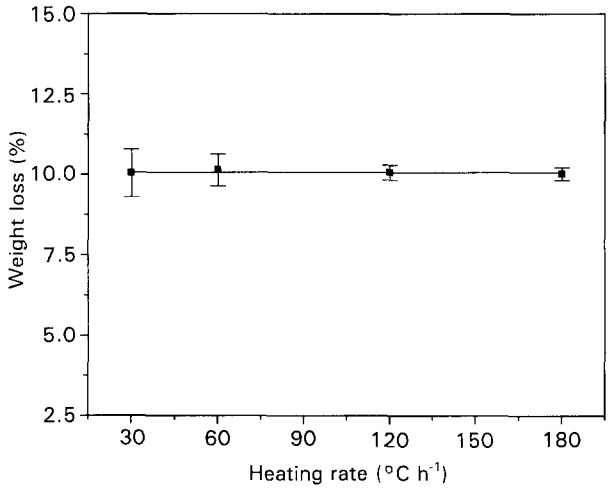

Figure 3 The weight loss of first-carbonized composites with different heating rates up to a carbonization temperature of 1000 °C.

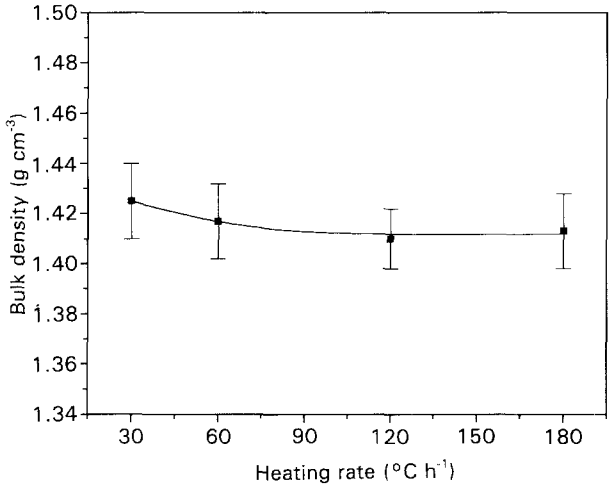

Figure 4 The bulk density of first-carbonized composites with different heating rates up to a carbonization temperature of 1000 °C.

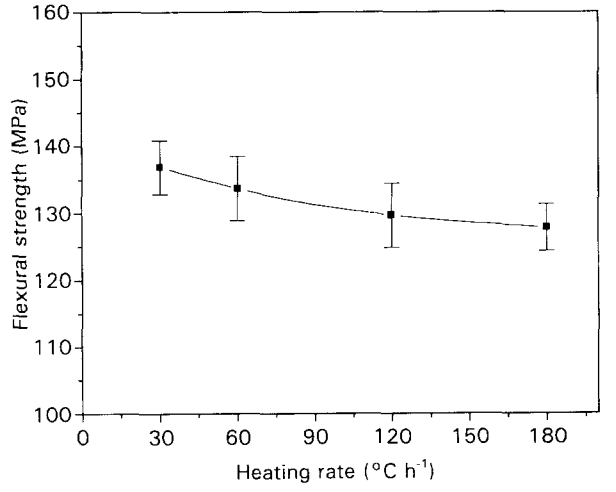

Figure 5 The flexural strength of first-carbonized composites with different heating rates up to a carbonization temperature of 1000 °C.

investigated. Figs 5 and 6 show the flexural strength and modulus, respectively, at various heating rates. Both the strength and modulus decrease with increasing heating rate. The presence of a void or crack in a composite can significantly reduce the mechanical

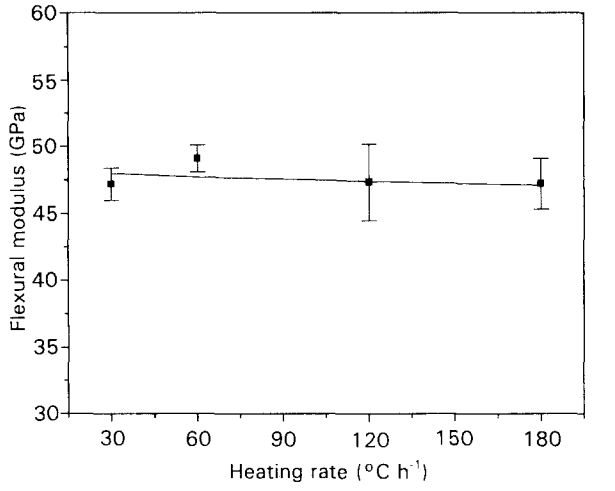

Figure 6 The flexural modulus of first-carbonized composites with different heating rates up to a carbonization temperature of 1000 °C.

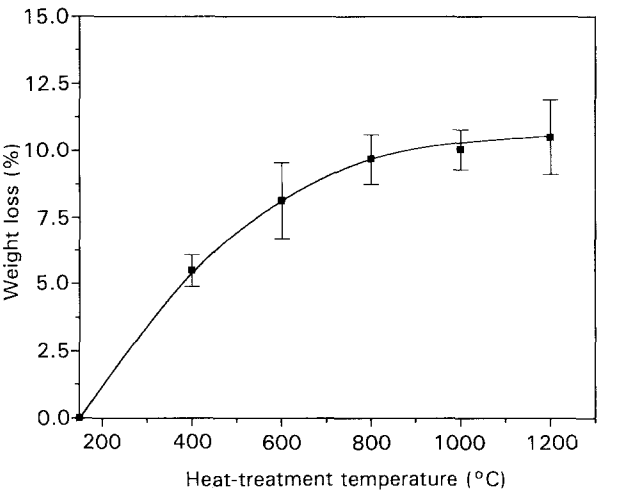

Figure 7 The weight loss of first-carbonized composites treated at various heat-treatment temperatures (heating rate = 30 °C h^{-1} in all cases).

properties of the composites. It was observed that the linear shrinkage resulting from the degradation reaction taking place within the composite matrix follows an inverse pattern to that of the density, which is correlated with the void content in the composites. The lower flexural strength of carbonized composites may be attributed to the formation of voids or cracks during the carbonization process.

3.1.2. Effect of heat-treatment temperature

3.1.2.1. Weight loss. The change in weight loss at various heat-treatment temperatures is illustrated in Fig. 7. The primary weight loss occurs during the treatment below 800 °C. At a temperature over 800 °C, the weight loss is relatively small because the evolution of the major pyrolysis products occurs below 800 °C.

3.1.2.2. Linear shrinkage. Fig. 8 shows the linear shrinkage of carbonized composites as a function of the heat-treatment temperature. A sharp increase in

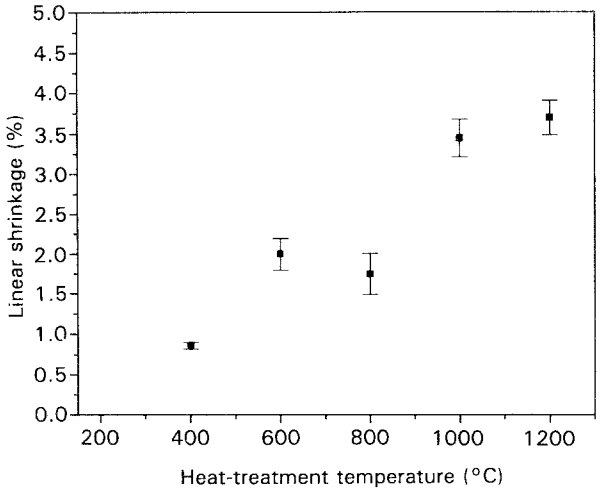

Figure 8 The linear shrinkage of first-carbonized composites treated at various heat-treatment temperatures (heating rate = 30 °C h^{-1} in all cases).

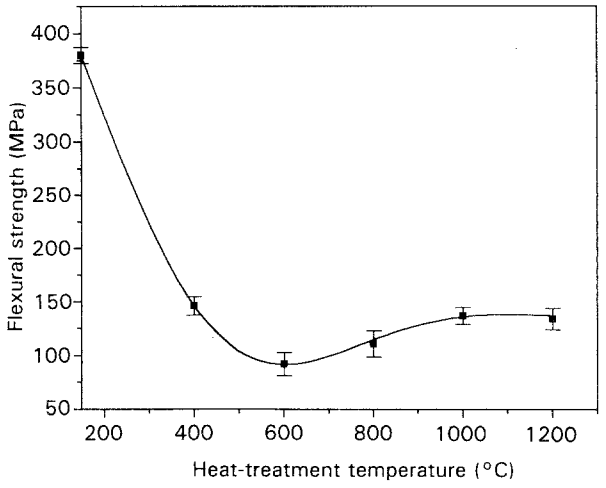

Figure 10 The flexural strength of first-carbonized composites treated at various heat-treatment temperatures (heating rate = 30 °C h^{-1} in all cases).

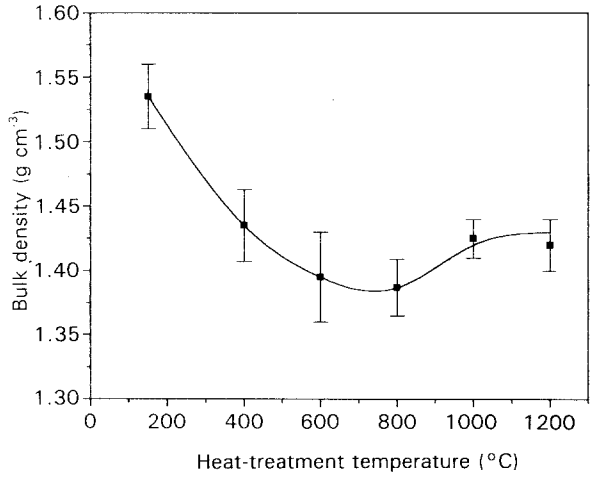

Figure 9 The density of first-carbonized composites treated at various heat-treatment temperatures (heating rate = 30 °C h^{-1} in all cases).

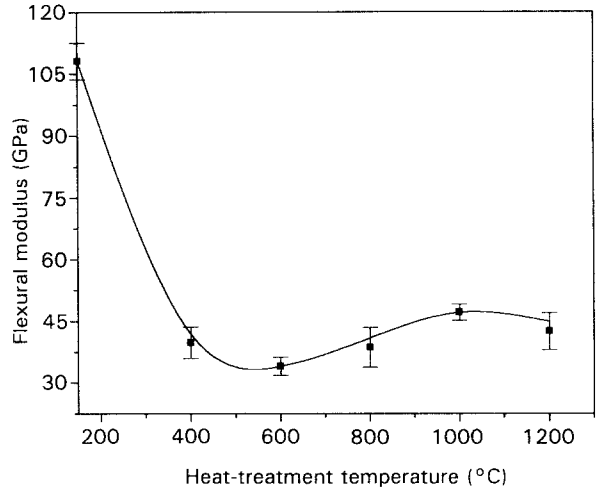

Figure 11 The flexural modulus of first-carbonized composites treated at various heat-treatment temperatures (heating rate = 30 °C h^{-1} in all cases).

linear shrinkage in the temperature range between 800 °C and 1000 °C is observed, although the weight loss in the same temperature range is insignificant. This may be due to the molecular rearrangement of the matrix to form a denser carbon matrix structure.

3.1.2.3. Density. Fig. 9 illustrates the density of carbonized composites treated at various temperatures. The density at the heat-treatment temperature, 1000 °C, is higher than that at 800 °C, although the weight loss is very similar in these two cases. A monotonic decrease in density of the carbonized composites in the temperature range between 150 and 800 °C is observed. This could be due to the crack formation within the composite during the evolution of voliate species in the carbonization process.

3.1.2.4. Flexural properties. The flexural strength and modulus of carbonized composites fabricated at various temperatures are illustrated in Figs 10 and 11, respectively. The flexural strength of the carbonized composites exhibits the lowest value at 600 °C, and then increases to about 140 MPa at 1200 °C. This result may be due to the formation of a denser carbon matrix at the higher heat-treatment temperature. The flexural modulus of the carbonized composites decreases rapidly during the initial carbonization treatment and increases slightly above 800 °C. The higher flexural modulus may also be attributed to the formation of the denser carbon matrix at the higher treatment temperature.

3.1.2.5. Morphology. Fig. 12 shows scanning electron micrographs which indicate the morphology change at the fracture surface of the carbonized composites. A wave-like structure in the matrix is observed in the composites in which the treatment temperature was over 800 °C. This structure may be one of the causes of the enhancement in flexural strength and modulus.

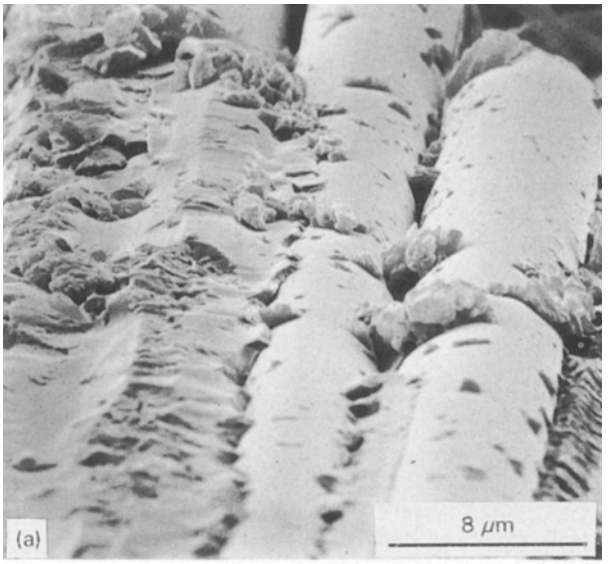

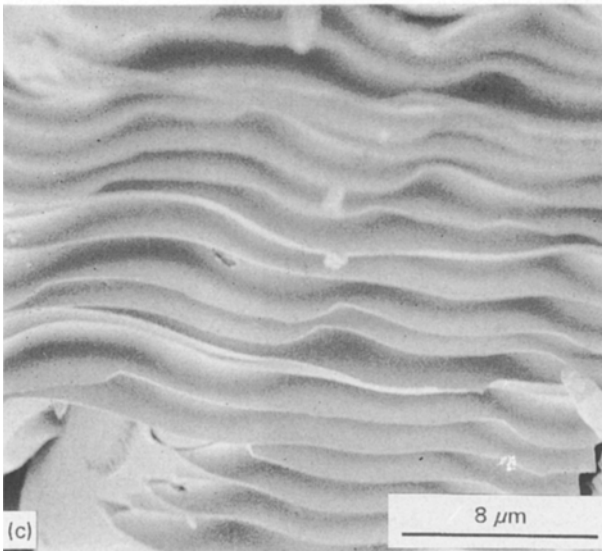

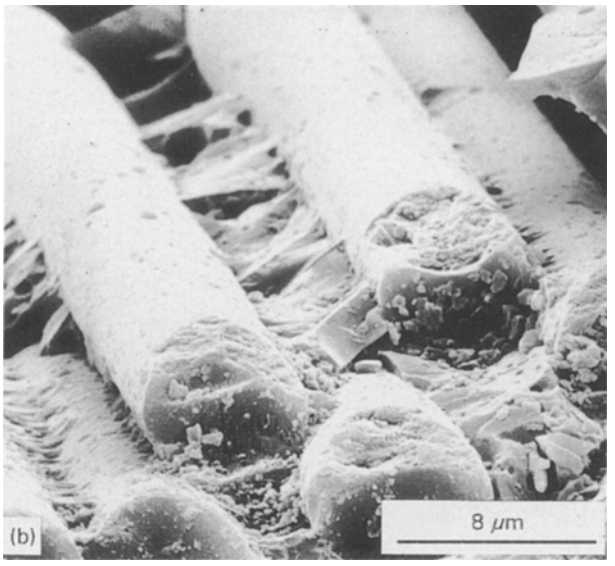

Figure 12 Scanning electron micrographs of the fracture surface of carbonized composites treated at different heat-treatment temperatures: (a) without heat treatment, (b) with heat treatment at 600 °C, (c) with heat treatment at 1000 °C.

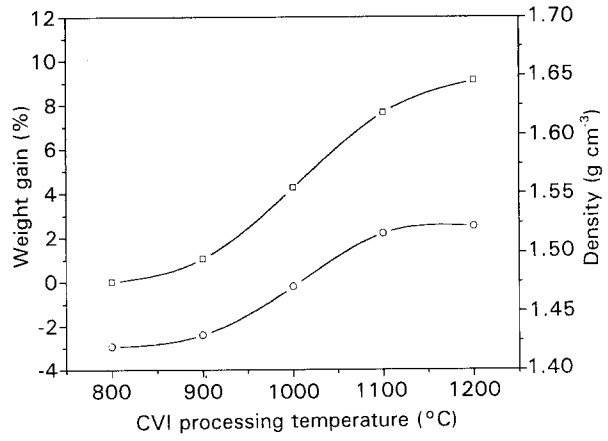

Figure 13 The (□) weight gain and (○) density of C/C composites densified by the CVI process at various deposition temperatures for 12 h.

3.2. Effect of densification treatment

3.2.1. Chemical vapour infiltration route

3.2.1.1. Weight gain and density change. Fig. 13 shows the weight gain and density change for composites fabricated by the chemical vapour infiltration process at various processing temperatures for 12 h. It was found that the higher the deposition temperature, the greater was the weight gain and the higher was the density. For specimens densified at a deposition temperature of 1200 °C, a severe deposition gradient was observed; a thick layer of carbon was deposited on the surface of composites as observed, whereas almost no deposition in the interior of the composite was detected. This is probably the reason why the density variation curve becomes flat as the processing temperature is increased.

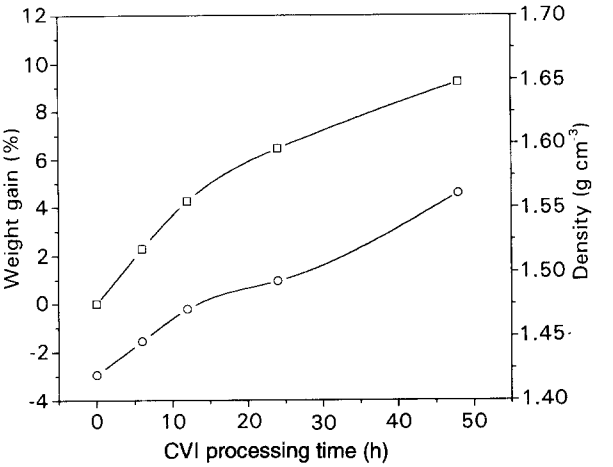

Figure 14 The (□) weight gain and (○) density of C/C composites densified by the CVI process at 1000 °C for various processing periods.

Fig. 14 shows the weight gain and density change for C/C composites densified by CVI at 1000 °C for various processing periods. It was found that the longer the processing periods, the greater was the weight gain and the higher was the density.

3.2.2. Resin-impregnation route

3.2.2.1. Weight gain and density change. Fig. 15 shows the weight gain and density change for composites fabricated by the liquid-resin impregnation

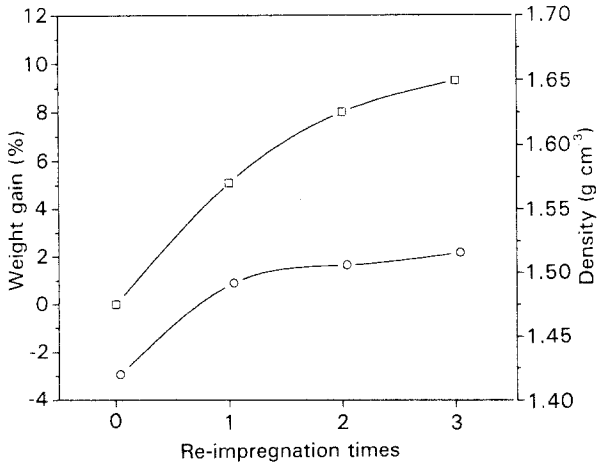

Figure 15 The (□) weight gain and (○) density of C/C composites densified by the resin re-impregnation process at various re-impregnation times.

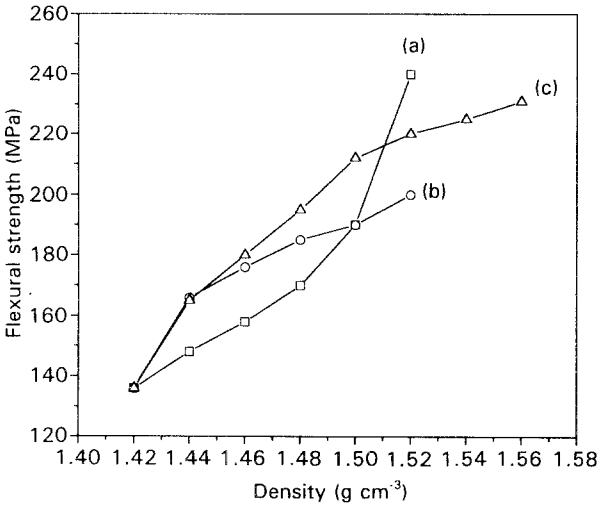

Figure 16 Flexural strength versus density of C/C composites densified by (a) the resin re-impregnation process, (b) the CVI process at various deposition temperatures for 12 h, and (c) the CVI process at 1000 °C for various deposition periods.

process. The increments in both the weight gain and density become smaller when the reimpregnation processes were repeated. The results imply that the number and size of the open pores are reduced as impregnation proceeds; moreover, the impregnation depth is also decreased if the applied pressure (near 1 atm in this study) is kept unchanged during impregnation. Furthermore, the increased rates of weight gain and density change are quite different after two resin impregnations.

3.2.3. Flexural properties

Curves a, b and c in Fig. 16 represent the relationship between flexural strength and density under various densification treatment conditions. It was found that the higher the density, the higher was the flexural strength. Among these three fabrication conditions, the increase in flexural strength under conditions a and c is more significant. Fig. 17 shows the relationship between flexural modulus and density under the same conditions as described. It is observed that a

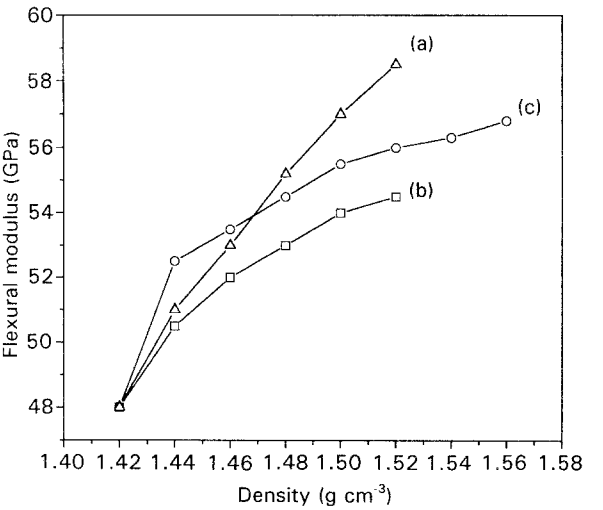

Figure 17 Flexural modulus versus density of C/C composites densified by (a) the resin re-impregnation process, (b) the CVI process at various deposition temperatures for 12 h, and (c) the CVI process at 1000 °C for various deposition periods.

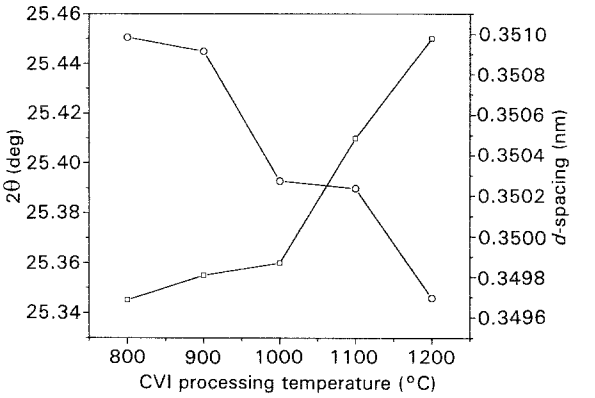

Figure 18 The (□) XRD 2θ and (○) *d*-spacing of C/C composites densified by the CVI process at various deposition temperatures for 12 h.

higher flexural modulus is obtained if a resin-impregnation process is applied.

3.2.4. Microstructure

Fig. 18 shows the interlayer spacing and diffraction peak of Bragg angles for composites fabricated by the CVI route at various deposition temperatures for 12 h. It is obvious that a more perfect structure can be obtained when a higher CVI processing temperature is applied.

Fig. 19 shows the gradient in thickness of the carbon deposited in the composites. The data are normalized by assuming that the deposition thickness at the outer surface of the C/C composites is 1. The deposition thickness was measured from an optical micrograph. Once a higher processing temperature is applied, the deposition gradient becomes larger due to a higher reaction rate at higher temperature; therefore, a significant species concentration consumption occurs during vapour infiltration; similar results were predicted by Tai and Chou [15] who proposed a deposition profile under various processing conditions for fabricating ceramic matrix composites by the CVI process.

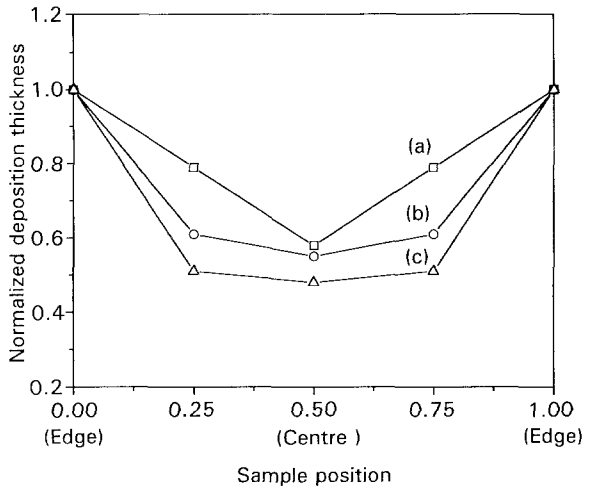

Figure 19 The deposition gradient within C/C composites fabricated by the CVI process at 1000 °C for (a) 12 h, (b) 24 h and (c) 48 h.

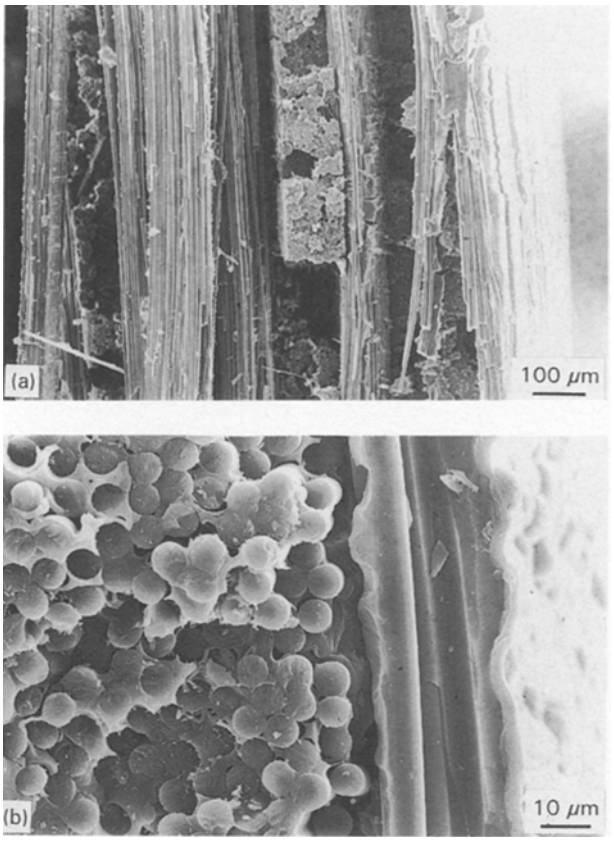

Figure 20(a, b) The fracture surface of the undensified C/C composites at different magnifications.

The interlayer spacing and diffraction peak of the Bragg angles for C/C composites fabricated by the resin-impregnation process do not change even after several impregnation treatments.

3.2.5. Morphology of the fracture surface

Fig. 20 shows scanning electron micrographs of the fracture surface of the undensified C/C composites. It is observed that fibre pull-out occurs at the fracture surface. This may be due to the voids around the fibres. Fig. 21 shows the fracture surface of the C/C composites densified by the CVI process. The fracture surface is smoother than that of the undensified C/C composites, which shows a catastrophic failure mode. The number of voids, as shown in Fig. 21b, is fewer than in the undensified C/C composites. The fracture surface of C/C composite densified through the CVI process shows a complex matrix morphology as indicated in Fig. 21b. The voids of the CVI densified C/C composites are fewer in number than in the undensified C/C composites, as seen by comparing Figs 21b and 20b.

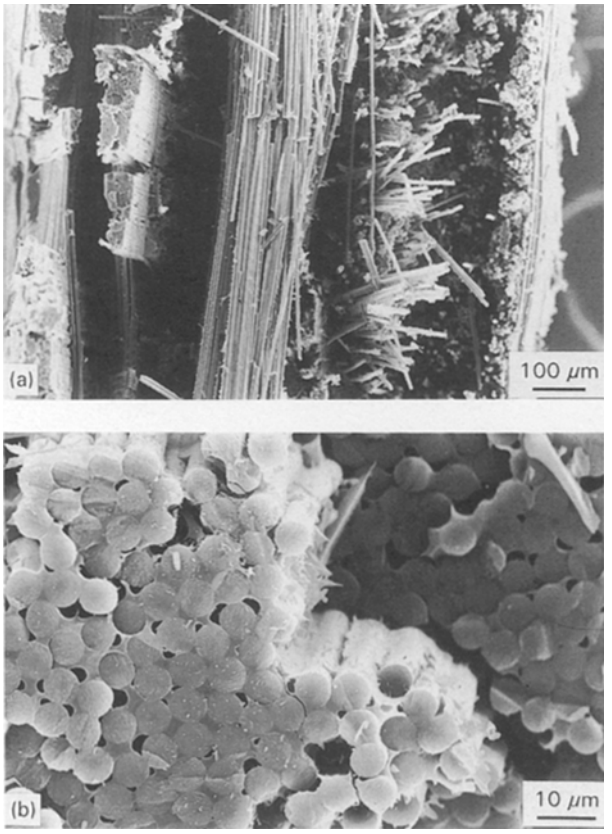

Figure 21(a, b) The fracture surface of C/C composities with CVI densification at different magnifications.

Fig. 22 shows the fracture surface of the C/C composites fabricated by the resin-impregnation method. A similar morphology of the fracture surface of the resin-impregnation method to that of the chemical vapour route is observed. The number of voids is also fewer than in undensified C/C composites, cf. Figs 20b and 22b.

3.2.6. Comparison of CVI route and the resin-impregnation route

The pore development in C/C composite during CVI may differ from that in the composite fabricated through liquid-impregnation. In the liquid-impregnation route, the pores were formed due to the pyrolysis shrinkage of the phenolic resin within composites; on the other hand, for composites fabricated by CVI, the pore size is reduced gradually due to the deposition of the solid product (carbon) on the pore surface.

The efficiency of these two methods for fabricating C/C composites is obvious when the density increment rate (density increment/total processing time) of

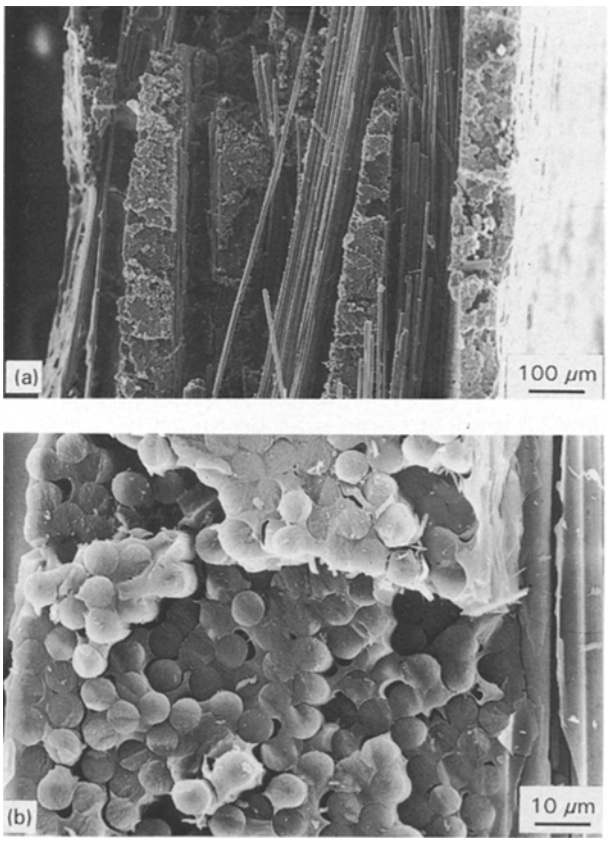

Figure 22(a, b) The fracture surface of C/C composites with liquid-resin impregnation densification at different magnifications.

the fabricated composite is measured. The density increases from 1.420 g cm^{-3} to 1.561 g cm^{-3} when the composites were densified by CVI at 1000 °C for 48 h; on the other hand, the density increases from 1.420 g cm^{-3} to 1.516 g cm^{-3} when the composites were densified by the liquid-resin impregnation route repeated for four times, and the processing period was 56 h for each impregnation. The total processing time of four re-impregnations is 224 h.

4. Conclusions

Densification of C/C composites by the CVI route as well as the liquid-resin impregnation route was performed. The results show that the carbonized composites have larger shrinkage and higher density when a lower heating rate for heat treatment is used. The flexural strength and modulus also increase slightly with lower heating rate. The flexural strength and modulus of C/C composites decrease when a higher treatment temperature up to 800 °C is applied; furthermore, the flexural strength and modulus of the composites increase when a treatment temperature up to 1200 °C is used. A higher flexural strength and flexural modulus can also be obtained after densification treatment because the densities of the specimens are increased by either one of these two fabrication methods. The interlayer spacing of the C/C composites is reduced as the processing temperature for CVI is increased. The deposition gradient of Pyro C within the preformed C/C composite becomes larger when the deposition temperature is increased. A different fracture morphology of the fracture surface of the densified composites and the undensified composites is also observed.

Acknowledgements

This research was financially supported by the National Science Council, Taiwan, under the contract NSC 81-0405-E-007-521.

References

1. E. FITZER, *Pure Appl. Chem.* **60** (1988) 287.
2. J. D. BUCKLEY, *Ceram. Bull.* **67** (1988) 364.
3. A. J. KLEIN, *Adv. Compos.* March/April (1989) 38.
4. C. F. LEWIS, *Mater. Eng.* January (1989) 27.
5. R. WEISS, in International Symposium on Carbon 1990, Tsukuba, Novermber 1990, edited by M. Inagaki (Carbon Society of Japan, Tokyo, 1990) Plenary C, pp. 10–15.
6. A. KELLY and S. T. MILEIKO, "Handbook of Composites", Vol. 4, "Fabrication of Composites" (Elsevier Science, Amsterdam, Netherlands, 1983) pp. 109–75.
7. S. MARINKOVIC, *Carbon* **29** (1991) 747.
8. M. K. ISMAIL, M. M. ROSE and M. A. MAHOWALD, *ibid.* **29** (1991) 575.
9. E. FIZER, *ibid.* **25** (1987) 163.
10. K. YANG, T. M. WU and C. P. CHANG, in "Proceedings of the 1986 Annual Conference of the Chinese Society for Material Science", Taichung, Taiwan, June 1986, edited by C. C. Lin (Chinese Society for Material Science, Tsing-Chu, Taiwan, 1986) pp. 147–61.
11. K. Y. SOHN, S. M. OH and J. Y. LEE, *Carbon* **26** (1988) 157.
12. T. H. KO and P. C. CHEN, *J. Mater. Sci. Lett.* **10** (1991) 301.
13. L. CHLOPEK and S. BLZEWICZ, *Carbon* **29** (1991) 127.
14. J. D. NAM and J. C. SEFERIS, *ibid.* **30** (1992) 751.
15. N. H. TAI and T. W. CHOU, *J. Am. Ceram. Soc.* **72** (1989) 414.

Received 22 October 1993
and accepted 16 May 1994